Structure and stability of helices in square-well homopolymers

M. N. Bannerman, J. E. Magee, and L. Lue*
School of Chemical Engineering and Analytical Science, The University of Manchester, P.O. Box 88, Sackville Street, Manchester M60 1QD, United Kingdom
(Received 21 May 2009; published 26 August 2009)

Recently, it has been demonstrated [Magee *et al.*, Phys. Rev. Lett. **96**, 207802 (2006)] that isolated square-well homopolymers can spontaneously break chiral symmetry and "freeze" into helical structures at sufficiently low temperatures. This behavior is interesting because the square-well homopolymer is itself achiral. In this work, we use event-driven molecular dynamics combined with an optimized parallel tempering scheme to study this polymer model over a wide range of parameters. We examine the conditions where the helix structure is stable and determine how the interaction parameters of the polymer govern the details of the helix structure. The width of the square well (proportional to λ) is found to control the radius of the helix, which decreases with increasing well width until the polymer forms a coiled sphere for sufficiently large wells. The helices are found to be stable for only a "window" of molecular weights. If the polymer is too short, the helix will not form. If the polymer is too long, the helix is no longer the minimum energy structure, and other folded structures will form. The size of this window is governed by the chain stiffness, which in this model is a function of the ratio of the monomer size to the bond length. Outside this window, the polymer still freezes into a locked structure at low temperature; however, unless the chain is sufficiently stiff, this structure will not be unique and is similar to a glassy state.

DOI: 10.1103/PhysRevE.80.021801 PACS number(s): 61.41.+e, 33.15.Bh

I. INTRODUCTION

One of the fascinating features of proteins is their ability to lock into a specific folded structure. This feature is often crucial to their function. A key structural unit which frequently appears in proteins is the helix. Helical structures also appear in other molecules, such as in DNA, homopolypeptides (e.g., polyalanine), as well as in some synthetic polymers. Consequently, there has been a lot of interest in the helix-coil transition as a starting point to understanding the more general issue of protein folding.

Many detailed computer simulations on "realistic" interaction potential models have been conducted to better understand the formation of helices in polypeptides and proteins (e.g., see Refs. [1–4]). In these systems, the formation of hydrogen bond interactions between different amino acid groups is principally responsible for the formation of the helix. Helices also spontaneously form in simplified interaction models that have short-ranged directional interactions between their constituent monomers [5,6]. Many theories have been developed to describe the helix-coil transition in homopolypeptides and other biological molecules, starting with the pioneering work of Zimm and Bragg [7] and later followed by many others [8–12]. The key feature of these theories is the characterization of a distinct helix and coil state for each residue in the peptide chain. This is justified for these systems because of the specific arrangement of the residues in the helix conformation and the large energies due to the formation of the hydrogen bonds. While these approaches have led to keen insights for helix formation in polypeptide and protein molecules, they are dependent on the fact that short-ranged directional interactions drive the formation of the helix structure. In these molecules, one can argue that the helix structure has been "built" in.

Can the helix structure occur in molecules without these specific interactions, and if so, what then controls its geometry? It has been suggested that the helix is a stationary configuration for semiflexible chains [13] and the optimal shape of flexible [14] and closely-packed compact [15,16] strings. This hints at a more general driving force for helix formation in real proteins and may explain why the structure is so prolific in nature. In order to gain some more general understanding of the mechanisms behind helix formation, we examine the square-well homopolymer model. This is a simple polymer model composed of linearly bonded hard spheres that interact with each other through an isotropic square-well attraction. Isolated square-well homopolymers exhibit the typical coil to globule transition observed in many polymers as the temperature is decreased below the theta point; however, they also freeze into compact crystal-like structures [17,18] at sufficiently low temperatures. Interestingly, Magee *et al.* [19] demonstrated that, by introducing stiffness, the square-well homopolymer model can fold into a helix structure. This is a remarkable result, as the model is achiral and yet it spontaneously breaks symmetry and folds into left- or right-handed helices. This is merely a result of the polymer being stiff, having an excluded volume and an attractive self interaction. An exact analysis of the density of states of square-well tetramers and pentamers was performed [20] to examine the relationship between the distributions and correlations of the torsional angles in these fragments to the stability of the helix in longer length chains. However, the question still remains as to what controls the geometry and the stability of the helical structures formed by these molecules.

In this work, we use molecular dynamics (MD) combined with the replica exchange method to explore the behavior of square-well homopolymers to better understand the link be-

*leo.lue@manchester.ac.uk

tween the interactions between the monomers of the chain and the overall structure of the molecule. In particular, we are interested in the range of conditions over which the helix structure is stable. The remainder of this paper is organized as follows. Section II describes the details of the square-well homopolymer model that we investigate in this work. In addition, it provides background information on the simulation methods we employed and outlines the procedures used to generate and analyze the resulting simulation data. The results of the simulations are presented in Sec. III. This section begins with an overview of the general behavior exhibited by the square-well homopolymers. Then, it continues by analyzing and discussing the influence of the bond length (or equivalently monomer size), the range of attraction between monomers, and the total number of monomers in the polymer on the structure and thermodynamic behavior of the homopolymer. Finally, the major findings of this work are summarized in Sec. IV.

II. SIMULATION DETAILS

The polymer model that we study in this work is a chain of linearly bonded monomers. Monomers that are not directly bonded together interact with each other through the potential

$$u(r) = \begin{cases} \infty & \text{for } r < \sigma \\ -\epsilon & \text{for } \sigma < r < \lambda\sigma \\ 0 & \text{for } \lambda\sigma < r, \end{cases} \quad (1)$$

where r is the distance between the centers of the monomers. Each monomer is a hard sphere of diameter σ surrounded by an attractive square well of diameter $\lambda\sigma$. When two monomers are within a distance $\lambda\sigma$, they feel an attractive interaction energy of magnitude ϵ. Monomers that are directly bonded together interact with each other through the potential

$$u_{\text{bond}}(r) = \begin{cases} \infty & \text{for } r < l - \delta \\ 0 & \text{for } l - \delta < r < l + \delta \\ \infty & \text{for } l + \delta < r. \end{cases} \quad (2)$$

The bond length is nominally equal to l but is allowed to fluctuate between $l-\delta$ and $l+\delta$. If $\sigma/l > 1$, then directly bonded monomers in the chain overlap. Monomers that are not directly bonded together other are not allowed to overlap each other. This induces a stiffness in the polymer due to the restrictions on the allowed bond angles imposed by the excluded volume interaction between monomers separated by two bonds. In the limit that σ/l approaches $2(1+\delta/l)$, the chain becomes completely rigid. For all the simulations presented here, $\delta/\sigma=0.1$, and so the bond length is allowed to vary by $\pm 10\%$. A schematic drawing of the polymer model is given in Fig. 1.

We use constant temperature MD to investigate the structural and thermodynamic properties of the square-well polymer chains over a range of temperatures. The temperature of the simulations was maintained with the Andersen thermostat [21]. The basic algorithm that we employ to perform the MD

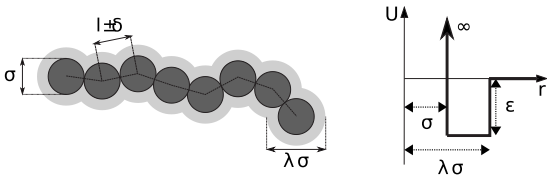

FIG. 1. Polymer model with bond length $l \pm \delta$, well energy ϵ, well width $\lambda\sigma$, and monomer diameter σ. The interaction energy between two nonbonded monomers separated by a distance r is given on the right.

simulations is based on the one originally developed by Alder and Wainwright [22]. Several subsequent advances have significantly improved the computational speed of this original algorithm. These include the use of overlapping cells [23,24], the delayed states algorithm [25], and calendar event queues [26]. We have incorporated these advances in order to construct a code where the computational cost of the simulation is independent of the number of particles N in the system.

One shortcoming of molecular dynamics is that it is prone to becoming trapped in local energy minima, especially at low temperatures. In particular for conditions where helical or other "frozen" structures are formed, the homopolymer may become locked within a specific configuration. Using only molecular dynamics, the helices formed by the square-well polymers are stable over the length of accessible simulation times and rarely transform between the left- and right-handed forms. This makes the study of the equilibrium behavior of these systems at low temperatures extremely formidable.

To overcome this difficulty, the MD simulations are coupled with the replica exchange/parallel tempering method [27]. In this technique, several molecular-dynamics simulations, each at a different temperature, are run simultaneously; a Monte Carlo move is added to exchange chain configurations between simulations at different temperatures. A configuration that is locked at a low temperature may then move up in temperature, unfold, and drop in temperature to sample another configuration. This enables the systems to rapidly overcome local energy minima and better explore the full range of available configurations.

The effectiveness of the replica exchange method depends on the choice of the temperatures of the individual simulations. In order to determine the optimal values of these temperatures, we use an approach recently developed by Katzgraber *et al.* [28]. This maximizes the number of configurations that travel between the lowest- and highest-temperature simulations, as modeled by a one-dimensional diffusion process. A typical optimal distribution of system temperatures is presented in Fig. 2, along with the resulting exchange rates. The optimization procedure clusters the simulation temperatures near conditions where the polymer undergoes structural changes with significant topological differences. The optimal distribution of system temperatures does not correspond to a constant acceptance ratio [28], as is commonly presumed.

A series of *NVT* molecular-dynamics simulations combined with the replica exchange method is performed to ex-

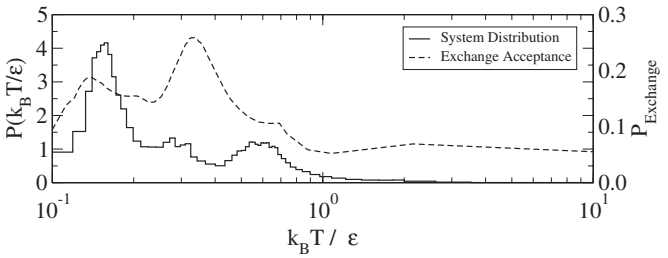

FIG. 2. Replica exchange simulations for an isolated square-well homopolymer with $N=20$, $\sigma/l=1.6$, and $\lambda=1.5$. Optimal distribution of system temperatures is given by the solid line, and the acceptance ratio of the replica exchange move for adjacent temperature systems is given by the dashed line.

amine the properties of square-well homopolymers over a range of values for σ/l, λ, and N. For each particular chain, 51 temperatures are used, and the systems are equilibrated for 10^4 attempted replica exchange moves. The replica exchange move consists of selecting 5×51 random pairs and attempting to swap the configuration between each pair. Between each replica exchange move, the dynamics of the isolated polymers is run for a few hundred mean free times. Following an initial equilibration period, data are collected over 5×10^4 attempted replica exchange moves. The collected data are then interpolated using multiple histogram reweighting [29] to obtain smooth heat-capacity curves as a function of the temperature.

III. RESULTS AND DISCUSSION

A. Overview

To illustrate the general behavior of the square-well homopolymers, we present results from MD simulations in Fig. 3 for a chain consisting of $N=20$ monomers with $\sigma/l=1.6$ and $\lambda=1.5$. The solid line in the plot shows the variation in the excess heat capacity C_v with temperature. The peaks of

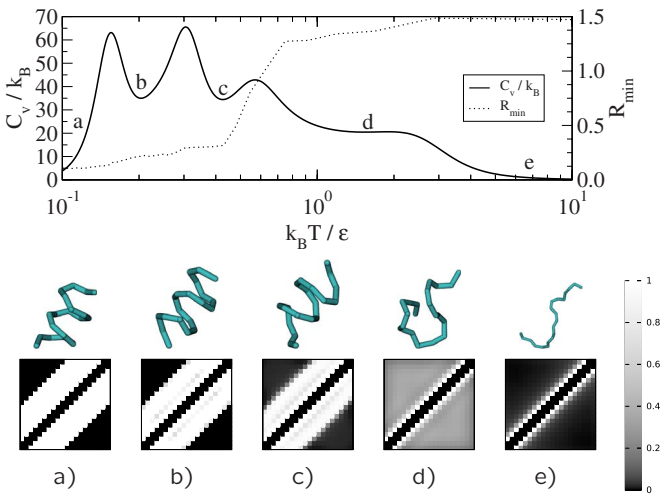

FIG. 3. (Color online) The heat capacity, the optimal configuration $D_{\rm rms}$, sample configurations, and contact maps at various temperatures $(a-e)$ of an isolated helix homopolymer with $N=20$, $\sigma/l=1.6$, and $\lambda=1.5$.

the heat capacity typically indicate transitions between different structural states of the polymer.

To characterize the rigidity (i.e., frozen vs flexible) of the structure of the homopolymer at a particular temperature, we collect N_{ss} configurations of the polymer at regular intervals in time during the course of the simulation (here we choose ten replica exchange times). For each sampled configuration α, we then determine the average R_α of the root-mean-square difference (rms, $D_{\rm rms}$) against all other collected configurations, which is given by

$$R_\alpha = N_{ss}^{-1}\sum_{\alpha'=1}^{N_{ss}} D_{\rm rms}(\alpha,\alpha'), \tag{3}$$

where the $D_{\rm rms}$ between two configurations α and α' is defined as

$$D_{\rm rms}(\alpha,\alpha') = \left[N^{-1}\sum_{i=1}^{N}|\mathbf{r}_i^{(\alpha)}-\mathbf{r}_i^{(\alpha')}|^2\right]^{1/2} \tag{4}$$

and $\mathbf{r}_i^{(\alpha)}$ is the position of monomer i in the polymer of configuration α. The reported value of the $D_{\rm rms}$ between a pair of configurations is the minimum value obtained by rotating [30] and reflecting the configurations, as well as reversing the numbering sequence of the monomers. We consider the configuration with the lowest value of R_α as the most representative of the entire set of sampled configurations of the homopolymer. The average $D_{\rm rms}$ of this configuration denoted by $R_{\rm min}$ is used to indicate how rigid the polymer structure is at a given temperature (i.e., $R_{\rm min}=\min_\alpha R_\alpha$). Low values of $R_{\rm min}$ suggest that the homopolymer remains frozen within the same structural configuration. High values of $R_{\rm min}$ indicate that the homopolymer is not well characterized by a single structure. This can imply that the homopolymer is in a rather flexible state, such as a coil or a molten globule. However, high values of $R_{\rm min}$ could also result if the homopolymer can be frozen into several distinct configurations, such as in a glassy state. Using cluster analysis of the distance matrix formed by the $D_{\rm rms}$'s of every pair of sample configurations, it is possible to estimate the number of stable states and thereby distinguish between these two situations. This issue will be discussed further in Sec. III D, where the effect of polymer length is explored.

The variation in $R_{\rm min}$ with temperature is given by the dotted line in the plot in Fig. 3. Beneath the plot are sample configurations of the homopolymer at several different representative temperatures. Underneath each of these configurations is the corresponding contact map of the average structure, which details the proximity of pairs of monomers in the polymer. The positions along the ordinate and abscissa of the contact maps denote each of the monomers along the chain. The locations within the contact map are shaded according to how often two monomers interact with each other (i.e., within a distance $\lambda\sigma$). Black denotes no interaction, white denotes continuous interaction, and gray denotes intermittent interaction. For monomers that are bonded together (along the diagonal), we have shaded the entries in the contact map black. For the case where $\sigma/l=1.6$ and $\lambda=1.5$,

monomers that are separated by two bonds are always in each others attractive well due to the overlap and result in two off-diagonal white bands.

At higher temperatures (point *e*), the polymer is extended, and the contact map indicates that the monomers of the polymer are rarely in contact with each other. The optimal configuration D_{rms} (R_{min}) also indicates that the typical configuration is not locked but, instead, is quite flexible. Upon decreasing the temperature, a shoulder in the heat capacity marks the transition from an extended coil to a globule state (point *d*). The contact map indicates that while monomers do interact significantly with each other, they do not remain in continuous contact with the same monomers, and therefore, the contact map is primarily gray. Although the polymer has collapsed into a compact structure, it contains no regular structure and R_{min} remains high.

Decreasing the temperature still further (point *c*), we see that the polymer changes from an unstructured globule to a more ordered helical structure. The contact map shows the stripe pattern that is characteristic of a spiral or helical structure. Two more helical structures are present at lower temperatures (points *b* and *a*) which possess a slightly different pitch and radius. The value of R_{min} decreases sharply over the first helix transition as the polymer forms a regular structure. This decreases further, indicating that the structures become more rigid. This is in agreement with the contact maps, where intermittent contacts become permanently "on" at low temperatures. Points *c* and *b* correspond to the helix 1 and 2 structures in the diagram of states presented by Magee *et al.* [19]. We will refer to the structure at point *a* as the helix 3 structure. The transitions between the three helical structures are not visible in R_{min} as the structures are very similar but the transition to a folded state is strongly marked.

In the following, we examine how the structure of square-well homopolymers is affected by the monomer size (σ/l), the range of the attractive interaction (λ), and the length of the polymer chain (N). In particular, we are interested in understanding the range of parameters where helical structures are stable.

B. Ratio of monomer size to bond length

In this section, we study the influence of monomer size, or equivalently the bond length, on the structure of square-well homopolymers. We limit our attention to homopolymers with $N=20$ and $\lambda=1.5$. The main effect of changing the monomer size is to alter the local stiffness of the polymer chain. Decreasing the size of the monomers (or increasing the bond length) increases the flexibility of the homopolymer. The stiffness of a polymer chain can be characterized by the bond correlation function, which is defined as

$$C(j)=\frac{1}{N-j-1}\sum_{k=1}^{N-j-1}\frac{\langle\Delta\mathbf{r}_k\cdot\Delta\mathbf{r}_{k+j}\rangle}{\langle\Delta\mathbf{r}_k\cdot\Delta\mathbf{r}_k\rangle}, \tag{5}$$

where $\Delta\mathbf{r}_k=\mathbf{r}_{k+1}-\mathbf{r}_k$ is the orientation of the kth bond in the polymer and $\mathbf{r}_k$ is the position of the kth monomer. This function describes the degree to which the orientations of two bonds are correlated with each other. The more flexible the chain, the more rapidly the bond correlation function decays with the distance j between the bonds.

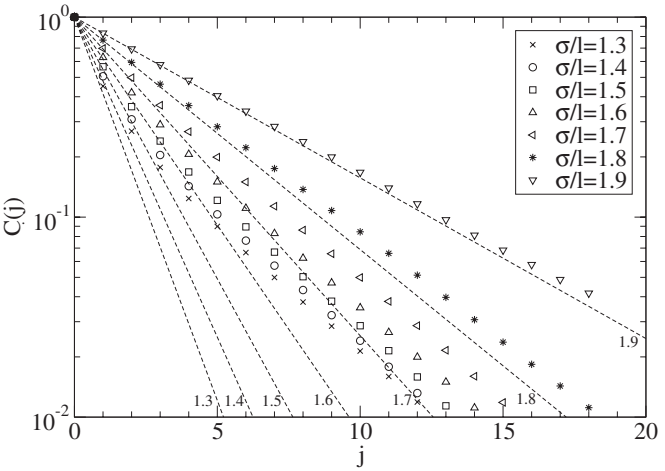

FIG. 4. Average bond angle correlations for athermal overlapping chains as a function of separation in a $N=20$ chain. The dotted lines correspond to neglecting the influence of long range excluded volume interactions between the monomers.

Figure 4 presents the bond correlation functions for athermal chains (i.e., $\epsilon=0$) with $N=20$ for various values of σ/l. The symbols are the results obtained from MD simulations. The dotted lines are the corresponding exponential decays for the athermal chains where excluded volume interactions are neglected, with the exception to those between monomers separated by two bonds, which give rise to the local stiffness. At very low values of σ/l (not shown), there are no correlations between the bonds, and the polymer behaves essentially as a random walk. At intermediate values of the overlap parameter, the excluded volume interactions between monomers separated by several bonds enhance the correlations between the bonds, and the correlation function decays algebraically rather than exponentially. For $\sigma/l>1.8$, the decay is nearly exponential because the chain is too stiff for there to be significant excluded volume interactions between the monomers.

A diagram of states for homopolymers with $N=20$ and $\lambda=1.5$ is given in Fig. 5, which explores the effect of the monomer overlap parameter (σ/l). The crosses mark the locations of peaks in the heat capacity, and the diagram is shaded according to the value of R_{min}. The data in Fig. 3 correspond to the vertical line at $\sigma/l=1.6$ in Fig. 5.

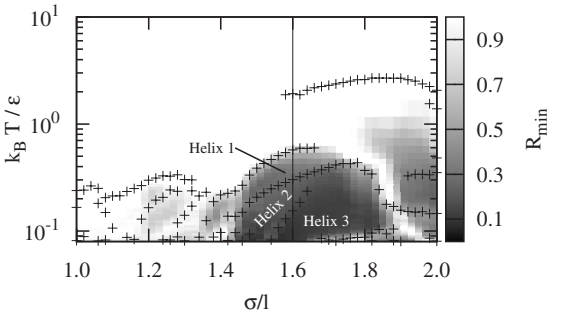

FIG. 5. Diagram of states for isolated square-well homopolymers with $N=20$ and $\lambda=1.5$. The graph is shaded according to R_{min}.

There are what at first appear to be discontinuities in the heat-capacity maxima in the diagram. These peaks are generally weak maxima in the heat capacity which are hidden behind the rapid increase in C_v due to the presence of sharper peaks at another temperature. The highest-temperature maximum in C_v typically corresponds to the coil-globule collapse or "theta point" (see point *d* in Fig. 3).

Homopolymers with $\sigma/l \lesssim 1.1$ crystallize into compact, nearly spherical, regularly packed structures at low temperatures [17,18]. The comparatively high value of the D_{rms} for these polymers, however, indicates that the structures that they freeze into are not unique. There may be several arrangements of the bonds of the polymer for a given "crystalline" packing of the monomers. Consequently, these polymers are like glasses at low temperatures.

When $\sigma/l \gtrsim 1+\delta/l=1.1$, directly bonded monomers always overlap one another. At low temperatures, homopolymers with $1.1 \lesssim \sigma/l \lesssim 1.4$ (see Fig. 5) exhibit a freezing transition; but, similarly to the polymers with $\sigma/l \lesssim 1.1$, they do not lock into a single stable conformation. The high value of the D_{rms} indicates that many folded configurations exist. On visual inspection of these configurations, helical features are visible within some other structure. For example, the ends of the polymer may be wrapped around the outside of a helical core. These "loose ends" increase the number of possible frozen states and therefore increase the value of R_{min}.

For homopolymers with a well width of $\lambda=1.5$, monomers separated by two bonds are permanently within each others attractive wells when $\sigma/l > 2(1+\delta/l)/\lambda \approx 1.47$. This coincides with the onset of the region of low values for R_{min}, where homopolymers fold into the helix 1, 2, and 3 structures. Here, the homopolymers fold into a single, helical conformation (neglecting the distinction between the left- and right-handed configurations). A significant portion of the folded parameter space is occupied by the helix 3 structure, which is the most rigid of the helix structures.

At high overlaps, the values of R_{min} are on average lower due to the stiffness of the chain limiting the range of motion of the monomers. There is a sharp transition at $\sigma/l \approx 1.8$ with an increase in R_{min} along the line of the heat-capacity peaks. For polymers with a well width of $\lambda=1.5$, two monomers separated by four bonds cannot interact with each other when $\sigma/l > \sqrt{7}/2 \approx 1.87$ [20]. If we account for the fact that in the simulations the bonds can stretch by 10%, then this would occur at $\sigma/l \gtrsim 1.70$, which coincides with loss of the helix 1 structure.

It appears that the observed helix structures are closely related to the constraint of interactions between monomers in the chain. The values at which certain interactions become prohibited depends on the well width λ, and the effect of this parameter is explored in the next section.

C. Range of attractive interaction

Now, we examine the influence of the range of the attractive interaction, which is characterized by the parameter λ. In this section, we limit the analysis to square-well homopolymers with $N=20$ and $\sigma/l=1.6$. A diagram of states is provided in Fig. 6. Several sample configurations are presented in Fig. 7 at various values of λ. From the diagram and the associated configurations, we see that a series of distinct helical structures are formed at low temperatures. The range of the attractive interaction appears to control the radius of the helix: smaller well widths lead to helical structures with a smaller radius and a larger pitch.

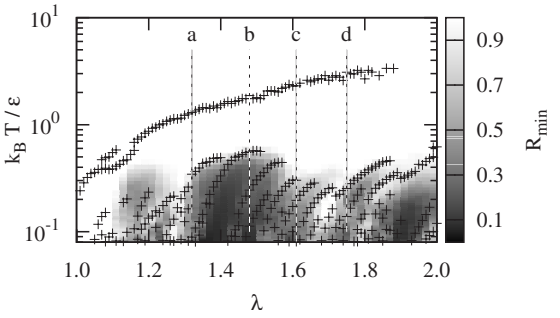

FIG. 6. Diagram of states for isolated square-well homopolymers with $N=20$ and $\sigma/l=1.6$. The graph is shaded according to R_{min}. The letters and dashed lines correspond to the configurations shown in Fig. 7.

At low values of the well width ($\lambda \lesssim 1.3$), helical structures appear with structural variations, much like what occurs at low values of the overlap parameter σ/l. For high values of λ, the helix structure begins to degrade. It still retains the spiral structure, however, it no longer has a constant radius. Interestingly, for the structure shown in Fig. 7(d), the monomers appear to be packed in a fairly spherical crystalline arrangement. If the well width becomes too large, then the helix structure will completely vanish, replaced by another structure.

For an overlap of $\sigma/l=1.6$ and a well width of $\lambda \geq 1.375$, monomers separated by two bonds are permanently within each others attractive well. This again coincides with a large decrease in R_{min}, indicating a single stable structure. As with the diagram of states in the overlap parameter σ/l (see Fig. 5), it is easy to distinguish certain helical structures using R_{min}.

It is interesting to note that the helices observed here all have a much higher monomer per turn count than the alpha helix commonly found in nature. There are 4 residues per turn of the alpha helix, whereas the wider helices presented here contain 7 for the tightest helix observed [Fig. 6(a)]. Maritan *et al.* [15] characterized their compact string helices using a parameter *f* related to the helix radius and monomer spacing in consecutive turns of the helix. Applying their analysis, the values of *f* exhibited by our helices are consistently above the value of $f \approx 1$ [e.g., Figs. 6(a)–6(d) $f \approx 1.2$,

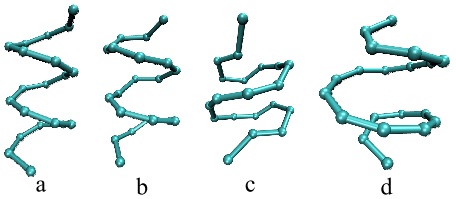

FIG. 7. (Color online) Representative configurations at the state points indicated in Fig. 6.

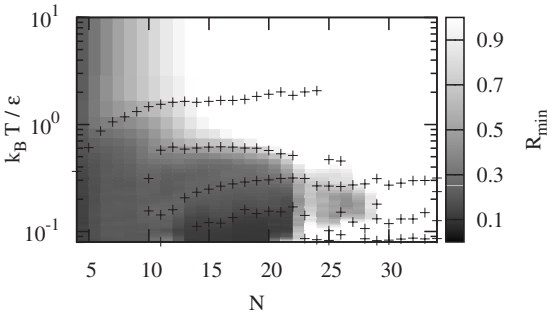

FIG. 8. Diagram of states for isolated square-well homopolymers with $\sigma/l=1.6$ and $\lambda=1.5$ as a function of the chain length N. The graph is shaded according to $R_{\min}$.

1.1, 1.3, and 1.1, respectively] reported by Maritan for compact strings and naturally occurring alpha helices. These larger values of f may be due to the manner in which we introduce stiffness (i.e., overlapping spheres).

Unlike the overlap parameter, the transitions between the various helical states are typically marked by peaks and large changes in $R_{\min}$, as the well-width parameter λ has a significant effect on the structure of the folded state. In the following section, we explore the structure as a function of chain length.

D. Chain length

For the square-well homopolymer, the main driving force for the formation of the helix is the tendency of the polymer to recover interaction energy through the contacts of its constituent monomers. This energetic driving force is balanced against the loss of entropy encountered in restricting the polymer to the helical structure (to maintain the necessary contacts). If the polymer chain is too short, then the energy recovered will not be sufficient to overcome the entropy loss, and the helix will not be stable. If the polymer chain is too long, then structures other than the helix are expected to be stable. Therefore, we expect the helix to appear only within a window of chain lengths. In this section, we examine the range of N where the helical structure is stable.

The diagram of states for square-well polymers with $\lambda=1.5$ and $\sigma/l=1.6$ is presented in Fig. 8. For small chain lengths ($N\lesssim 12$) the $D_{\rm rms}$ is, on average, a low value. This is due to the short distance that monomers can actually be separated in space. This can be accounted for by reducing $R_{\min}$ by the chain length; however, similar structures at different chain lengths typically exhibit the same value of $R_{\min}$ and these data would be lost. The conditions where helical structures are formed are still well defined by the heat-capacity peaks and areas where the value of $R_{\min}$ is low. For this system, the chain must consist of at least $N=10$ monomers before helices can form. The helix 3 structure does not appear until $N=14$, and the largest chain length, at which the helix structure is stable, is $N=22$.

At low temperatures, homopolymers with $N>22$ appear to freeze into rigid structures yet the high values of $R_{\min}$ indicate that the homopolymer does not freeze into a single repeatable folded structure. In fact, these folded states are no longer unique, and several distinct structures exist with comparable free energies. These longer homopolymers arrange themselves into regularly packed structures with a spherical shape. Figure 9 provides several snapshots of configurations for square-well homopolymers with $N=34$ at a temperature $k_BT/\epsilon=1.35$ (see also Fig. 8). These chiral structures have the same interaction energy, and they are all stable over long times. They appear to be variations in a similar structural theme: a core of a few monomers with a chiral outer core.

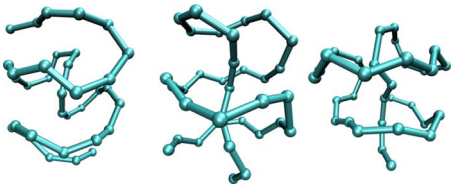

FIG. 9. (Color online) Samples of stable configurations for square-well homopolymers with $\sigma/l=1.6$, $\lambda=1.5$, and $N=34$ at $k_BT/\epsilon=0.137\,41$.

The $D_{\rm rms}$'s of the different folded structures in Fig. 9 lie between 0.86σ and 1.05σ, which is a relatively high value. Thus, the $D_{\rm rms}$ can discriminate between distinct folded structures provided that the configurations within each of the structures have a low average $D_{\rm rms}$. If we perform a quality threshold (QT) cluster analysis [31] of the $D_{\rm rms}$ between all pairs of sample configurations using a cut-off value of $<0.25\sigma$ to group the data and a threshold of 1% to eliminate intermediates, we can attempt to count the number of distinct structures formed. We perform this counting at the heat-capacity minima as the heat-capacity maxima tend to occur at transitions between structures. For $N=22$, only one cluster is apparent, which indicates that the homopolymer folds into a unique structure at low temperatures; in this case, it is a helix. In contrast, for $N=23$, a single helix occupies approximately 50% of the simulation snapshots. The remainder are a large number of variations on the helix with loose ends wrapped around the central coil.

In fact, once the single helix structure is no longer dominant the number of distinct folded structures rapidly increases with the length of the homopolymer. These polymers will behave similarly to a glass at low temperatures, becoming trapped into one of these many structures.

To understand how the range of the attractive interactions affects the window of chain lengths where the helix is stable, we examine square-well homopolymer chains with $\lambda=1.32$ and $\sigma/l=1.6$. The diagram of states is presented in Fig. 10. These polymers tend to form helices at shorter chain lengths than polymers with a wider well widths (cf. Fig. 8 for $\lambda=1.5$). The helices formed by the $\lambda=1.32$ polymers have a tighter radius and are more rigid (lower value of $R_{\min}$) than the helices formed by the $\lambda=1.5$ polymers. The shortest homopolymer that forms a helix ($N=8$) appears to be correlated with the number of monomers in a single turn of the helix. The helix structure vanishes for chain lengths greater than $N=22$, which is similar to what is found for homopolymers with $\lambda=1.5$. At longer chain lengths, the system again exhibits multiple folded states, and the structures formed are similar to those displayed in Fig. 9.

To investigate the influence of the monomer size (or bond length) on the window of chain lengths where the helix is

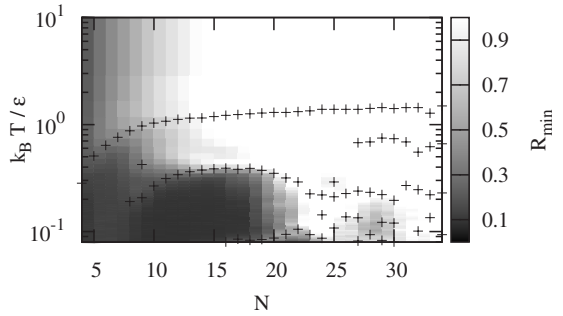

FIG. 10. Diagram of states for isolated square-well homopolymers with $\sigma/l=1.6$ and $\lambda=1.32$ as a function of the chain length N. The graph is shaded according to $R_{\min}$.

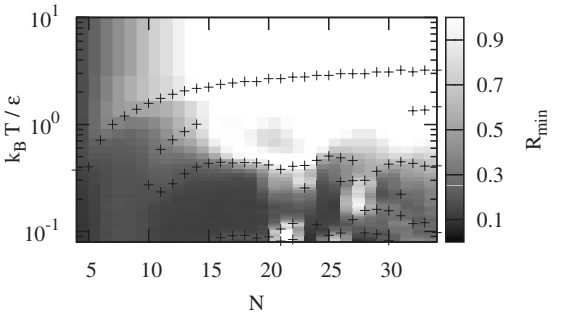

FIG. 11. Diagram of states for isolated square-well homopolymers with $\sigma/l=1.8$ and $\lambda=1.5$ as a function of the chain length N. The graph is shaded according to $R_{\min}$.

formed, we examine square-well homopolymers with $\sigma/l=1.8$ and $\lambda=1.5$. The diagram of states for these systems is given in Fig. 11, which shows a rich range of structural behavior. The minimum chain length for helix formation is larger ($N=11$) than for polymers with a monomer size of $\sigma/l=1.6$. The increased stiffness of the chain is limiting the curvature of the helix formed, thus requiring more monomers per turn of the helix. It appears that the typical "glassy" behavior of the longer polymers has been eliminated for the examined chain lengths. Therefore, the maximum chain length displaying a helical structure must be determined using QT analysis and visual inspection. The last chain length where a single helix structure is stable is $N=22$, yet for the longer chain lengths ($23 \leq N \leq 34$), the folded structures remain unique and not glassy. A single structure, which we refer to as the "barbers pole" structure, is observed over these chain lengths and is similar to the two rightmost structures of Fig. 9. This structure was first observed by Magee *et al.* (see Fig. 2 of Ref. [19]). Unlike the configurations of Fig. 9, the polymer is too stiff to allow the reversal of direction or doubling back of the outer spiral in the barbers pole. It appears that the increased stiffness has reduced the number of possible low-energy permutations, which manifest in more flexible chains as the doubling back of the outer spiral, to a single configuration. The small regions of high $R_{\min}$ at low temperatures in Fig. 11 correspond to broad peaks in the heat capacity where transitions between different barbers pole structures occur.

Chains with a higher value of σ/l appear to favor a single-folded structure at longer chain lengths than compared to more flexible chains. This is understandable as in the limit of a rigid chain there is only one possible physical configuration. As the chain becomes stiffer the number of low-energy permutations on a structural theme are limited until only one configuration becomes optimal.

IV. CONCLUSIONS

In this work, we have used event-driven molecular dynamics, coupled with the replica exchange and histogram reweighting techniques, to explore the behavior of isolated square-well homopolymers. The structural properties of these polymers were characterized through a combination of configurational snapshots, monomer contact maps, and the root-mean-square deviation of the configuration combined with QT cluster analysis. The $D_{\rm rms}$ is able distinguishing between the unfolded and folded helix states. QT cluster analysis of the $D_{\rm rms}$ allows the estimate of the number of folded states, which reflects the "variability" of the state.

The homopolymer model studied here exhibits complex behavior. The stability of the helix structure is related to the constriction/elimination of interactions between monomers separated by a number of bonds in the chain. This is affected by the chain stiffness, which controlled by the monomer overlap parameter σ/l. The pitch and curvature of a helix is governed mainly by the range of the attractive interaction λ. Helices form with a higher curvature for short-range attractive wells. For larger values of λ, the monomers pack into a more spherical arrangement while still retaining a spiral bond structure.

Helices are only stable within a window of the chain length N. The lower limit appears to be related to the number of monomers in a single turn of the stable helix structure. Above a critical chain length, the isolated homopolymer folds into a rapidly increasing number of stable states, displaying characteristics reminiscent of a glass transition. These structures are more compact and spherical than their lower N counterparts, result from a minimization of the surface area to volume ratio of the polymer.

Finally, as the stiffness of the homopolymer is increased $[\sigma/l \rightarrow 2(1+\delta/l)]$ the number of observed folded states in longer chain lengths is reduced. At an overlap of $\sigma/l=1.9$, we only observe unique folded states for the range of polymer lengths studied ($4 \leq N \leq 34$).

ACKNOWLEDGMENT

M.N.B. acknowledges support from an EPSRC DTA.

[1] Y. Okamoto and U. Hansmann, J. Phys. Chem. **99**, 11276 (1995).
[2] C. L. Brooks, Acc. Chem. Res. **35**, 447 (2002).
[3] H. D. Nguyen, A. J. Marchut, and C. K. Hall, Protein Sci. **13**, 2909 (2004).
[4] H. A. Scheraga, M. Khalili, and A. Liwo, Annu. Rev. Phys. Chem. **58**, 57 (2007).
[5] J. P. Kemp and Z. Y. Chen, Phys. Rev. Lett. **81**, 3880 (1998).
[6] J. P. Kemp and J. Z. Y. Chen, Biomacromolecules **2**, 389 (2001).
[7] B. H. Zimm and J. K. Bragg, J. Chem. Phys. **31**, 526 (1959).
[8] S. Lifson and A. Roig, J. Chem. Phys. **34**, 1963 (1961).
[9] V. Varshney, T. E. Dirama, T. Z. Sen, and G. A. Carri, Macromolecules **37**, 8794 (2004).
[10] J. A. Schellman, J. Chem. Phys. **62**, 1485 (1958).
[11] V. Munoz and L. Serrano, Nat. Struct. Biol. **1**, 399 (1994).
[12] A. J. Doig, Biophys. Chem. **101-102**, 281 (2002).
[13] A. Kholodenko, M. Ballauff, and M. A. Granados, Physica A **260**, 267 (1998).
[14] T. Vogel, T. Neuhaus, M. Bachmann, and W. Janke, EPL **85**, 10003 (2009).
[15] A. Maritan, C. Micheletti, A. Trovato, and J. Banavar, Nature (London) **406**, 287 (2000).
[16] D. Marenduzzo, A. Flammini, A. Trovato, J. Banavar, and A. Maritan, J. Polym. Sci., Part B: Polym. Phys. **43**, 650 (2005).
[17] Y. Zhou, C. K. Hall, and M. Karplus, Phys. Rev. Lett. **77**, 2822 (1996).
[18] Y. Zhou, M. Karplus, J. Wichert, and C. Hall, J. Chem. Phys. **107**, 10691 (1997).
[19] J. E. Magee, V. R. Vasquez, and L. Lue, Phys. Rev. Lett. **96**, 207802 (2006).
[20] J. E. Magee, L. Lue, and R. A. Curtis, Phys. Rev. E **78**, 031803 (2008).
[21] H. C. Andersen, J. Chem. Phys. **72**, 2384 (1980).
[22] B. J. Alder and T. E. Wainwright, J. Chem. Phys. **31**, 459 (1959).
[23] D. C. Rapaport, J. Comput. Phys. **34**, 184 (1980).
[24] A. T. Krantz, ACM Trans. Model. Comput. Simul. **6**, 185 (1996).
[25] M. Marin, D. Risso, and P. Cordero, J. Comput. Phys. **109**, 306 (1993).
[26] G. Paul, J. Comput. Phys. **221**, 615 (2007).
[27] R. H. Swendsen and J. S. Wang, Phys. Rev. Lett. **57**, 2607 (1986).
[28] H. G. Katzgraber, S. Trebst, D. A. Huse, and M. Troyer, J. Stat. Mech.: Theory Exp. (2006), P03018.
[29] A. M. Ferrenberg and R. H. Swendsen, Phys. Rev. Lett. **63**, 1195 (1989).
[30] W. Kabsch, Acta Crystallogr., Sect. A: Cryst. Phys., Diffr., Theor. Gen. Crystallogr. **32**, 922 (1976).
[31] L. J. Heyer, S. Kruglyak, and S. Yooseph, Genome Res. **9**, 1106 (1999).